

# Ab Initio Calculation of Finite Temperature Charmonium Potentials

P.W.M. Evans<sup>a</sup>, C.R. Allton<sup>a</sup> and J.-I. Skullerud<sup>b</sup>

<sup>a</sup>*Department of Physics, Swansea University, Swansea, United Kingdom*

<sup>b</sup>*Department of Mathematical Physics, National University of Ireland Maynooth*

*Maynooth, County Kildare, Ireland*

(Dated: July 15, 2018)

The interquark potential in charmonium states is calculated for the first time in both the zero and non-zero temperature phases from a first-principles lattice QCD calculation. Simulations with two dynamical quark flavours were used with temperatures  $T$  in the range  $0.4T_c \lesssim T \lesssim 1.7T_c$ , where  $T_c$  is the deconfining temperature. The correlators of point-split operators were analysed to gain spatial information about the charmonium states. A method, introduced by the HAL QCD collaboration and based on the Schrödinger equation, was applied to obtain the interquark potential. We find a clear temperature dependence, with the central potential becoming flatter (more screened) as the temperature increases.

PACS numbers: 11.10.Wx, 12.38.Gc, 14.40.Pq

*Introduction* – The quark-gluon plasma (QGP) phase of QCD has been studied extensively both in heavy-ion collision experiments at RHIC [1, 2] and the LHC [3] as well as in theoretical calculations. However, a complete understanding of this phase is still some distance away. Experiments are hindered by uncertainties in the phenomenology of the QGP such as the equation of state, transport properties, and spectral features of hadrons. These quantities are required to model the QGP fireball in heavy-ion collisions as it expands and cools back into the hadronic phase in order that the events in the detectors can be properly interpreted.

One of the quantities of interest is the interquark potential in the QGP phase. A temperature dependent charmonium potential underlies the widely cited  $J/\psi$  suppression model of Ref. [4]. More recent work on statistical models of charmonium production [5, 6] and studies assuming transport models of charmonium production [7, 8] lead to alternative interpretations. An analogous suppression has recently been found in bottomonium yields in heavy-ion collisions [9, 10].

Theoretical work on the interquark potential at high temperature includes early models [11] and perturbative QCD calculations [12]. Furthermore, there have been some recent non-perturbative (i.e. lattice) QCD studies of interquark potentials which are relevant to the work presented here. These fall into two categories: (i) non-zero temperature studies of the *static* quark potential [13–17] and (ii) *zero temperature* studies of the potential between quarks with finite masses [18]. The work presented here is a study of the interquark potential of charmonium using *physical charm quark masses* at *finite temperature* and uses two flavours of light dynamical quark. A particular feature of our work is that our lattices are anisotropic which has the significant advantage that our correlation functions are determined at a large number of temporal points, hence aiding our analysis.

The method we use is based on the HAL QCD collaboration’s calculation of the *internucleon* potential relevant for nuclear physics and utilised the Schrödinger equation

[19]. In this work we use their “time-dependent” method [20] to determine the real part of the *interquark* charmonium potential. In our work we do not consider the width of the state and therefore have access to the real part of the potential only. The possible limitations of the underlying assumption, that a nonrelativistic potential description is valid for these temperatures and quark masses, is a separate issue which will not be discussed here.

Our main conclusion is that the charmonium potential as a function of distance is steepest for low temperatures  $T$ , and becomes flatter at large distances as  $T$  increases. This work extends our earlier work in [21].

*Time-dependent Schrödinger Equation Approach* – Following HAL QCD, we determine the potential using their “time-dependent” method [20]. The first step is to define charmonium point-split operators,

$$J_\Gamma(x; \mathbf{r}) = q(x) \Gamma U(x, x + \mathbf{r}) \bar{q}(x + \mathbf{r}), \quad (1)$$

where  $\mathbf{r}$  is the displacement[31] between the charm and anti-charm quark fields  $q$  and  $\bar{q}$ ,  $x$  is the space-time point  $(\mathbf{x}, \tau)$  and  $\Gamma$  is a Dirac matrix used to generate vector ( $J/\psi$ ) or pseudoscalar ( $\eta_c$ ) channels.  $U(x, x + \mathbf{r})$  is the gauge connection between  $x$  and  $x + \mathbf{r}$ . The correlation functions,

$$C_\Gamma(\mathbf{r}, \tau) = \sum_{\mathbf{x}} \langle J_\Gamma(\mathbf{x}, \tau; \mathbf{r}) J_\Gamma^\dagger(0; \mathbf{0}) \rangle. \quad (2)$$

of the point-split and local operators, can be expressed in the usual spectral representation,

$$C_\Gamma(\mathbf{r}, \tau) = \sum_j \frac{\psi_j^*(\mathbf{0}) \psi_j(\mathbf{r})}{2E_j} \left( e^{-E_j \tau} + e^{-E_j(N_\tau - \tau)} \right), \quad (3)$$

where the sum is over the states  $j$  with the same quantum numbers as the operator  $J_\Gamma$ , and  $\psi_j(\mathbf{r})$  are the corresponding Nambu Bethe Salpeter (NBS) wavefunctions.  $N_\tau$  is the number of lattice points in the temporal direction and is related to the temperature by  $T = 1/(a_\tau N_\tau)$ , where  $a_\tau$  is the temporal lattice spacing.

From now on we consider only radially symmetric (S-wave) states. We differentiate Eq.(3) w.r.t. time and apply the Schrödinger equation which, in Euclidean space-time is

$$\left[ -\frac{1}{2\mu} \frac{\partial^2}{\partial r^2} + V_\Gamma(r) \right] \psi_j(r) = E_j \psi_j(r), \quad (4)$$

where  $\mu$  is the reduced mass of the  $c\bar{c}$  system,  $\mu = \frac{1}{2}m_c \simeq \frac{1}{4}M_{J/\psi}$ . Ignoring the backward moving contribution, we obtain

$$\begin{aligned} \frac{\partial C_\Gamma(r, \tau)}{\partial \tau} &= \sum_j \left( \frac{1}{2\mu} \frac{\partial^2}{\partial r^2} - V_\Gamma(r) \right) \frac{\psi_j^*(0)\psi_j(r)}{2E_j} e^{-E_j\tau} \\ &= \left( \frac{1}{2\mu} \frac{\partial^2}{\partial r^2} - V_\Gamma(r) \right) C_\Gamma(r, \tau). \end{aligned} \quad (5)$$

This can be trivially solved for the potential  $V_\Gamma(r)$ .

Notice that the NBS wavefunction,  $\psi(r)$ , is not explicitly required in the above derivation of  $V(r)$ . However, we note that HAL QCD's original ‘‘wavefunction’’ method extracts  $\psi(r)$  from a fit to the large time behaviour of the correlation function,  $C(r, \tau) \rightarrow \psi_0(0)\psi_0(r) e^{-E_j\tau}$ , and then uses this  $\psi_0(r)$  as input into the Schrödinger equation to obtain the potential [18]. HAL QCD's time-dependent method used here has the distinct advantage that the correlation functions are used directly, without requiring a fit to the asymptotic state.

The S-wave potential can be expressed as

$$V_\Gamma(r) = V_C(r) + \mathbf{s}_1 \cdot \mathbf{s}_2 V_S(r), \quad (6)$$

where  $V_C$  is the spin-independent (or ‘‘central’’) potential,  $V_S$  is the spin-dependent potential, and  $\mathbf{s}_{1,2}$  are the spins of the quarks. We have  $\mathbf{s}_1 \cdot \mathbf{s}_2 = -3/4, 1/4$  for the pseudoscalar and vector channels respectively.

*Lattice Parameters and Correlators* – We performed lattice calculations of QCD with two dynamical flavours of light quark using a Wilson-type action with anisotropy of  $\xi = a_s/a_\tau = 6$ ,  $a_s \simeq 0.162\text{fm}$  and  $a_\tau^{-1} \simeq 7.35\text{GeV}$  [22, 23]. The other lattice parameters are listed in Table I. We note that the range of temperatures is from the confined phase up to  $\sim 1.7T_c$  where  $T_c$  is the deconfining transition. The charm quark is simulated with the (anisotropic) clover action and its mass is set by matching the experimental  $\eta_c$  mass at zero temperature.

$N_s$	$N_\tau$	$T(\text{MeV})$	$T/T_c$	$N_{\text{cfg}}$
12	80	90	0.42	250
12	32	230	1.05	1000
12	28	263	1.20	1000
12	24	306	1.40	500
12	20	368	1.68	1000

TABLE I: Lattice parameters used, including spatial and temporal dimension,  $N_s$  and  $N_\tau$ , temperature, and number of configurations,  $N_{\text{cfg}}$ .

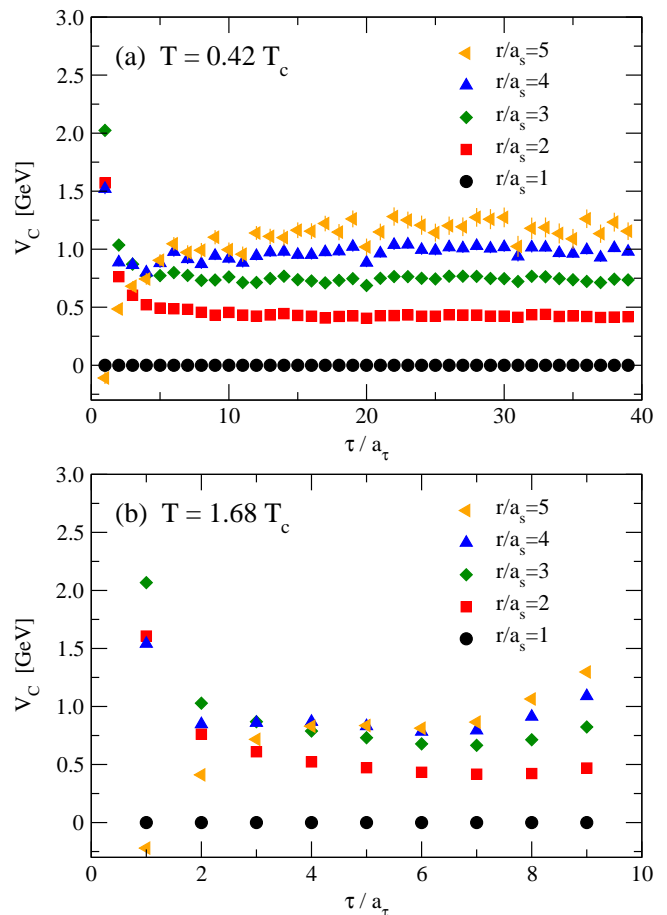


FIG. 1: The results for the central potential  $V_C(r)$  obtained from Eq. (5) for (a)  $T = 0.42T_c$  and (b)  $1.68T_c$ . The horizontal axis is the Euclidean time,  $\tau$ , appearing in Eq. (5)

*Results* – We now apply Eq. (5) to obtain the potential,  $V_\Gamma(r)$ , for the temperatures listed in Table I for the vector and pseudoscalar channels separately. In Eq. (5), standard symmetric lattice finite differences are used for the spatial and temporal derivatives. Figure 1 shows the central potential obtained for  $T/T_c = 0.42$  and  $1.68$  as a function of the time,  $\tau$ , appearing in Eq. (5). For each  $\tau$  value in Fig.1, we have vertically shifted the data points so that  $V_C(r/a_s = 1) = 0$ .

As can be seen, there is a good plateau where the potential  $V_C(r)$  is stable. The lack of a plateau at small times is presumably due to lattice artefacts caused by contact terms at the source. The upward trend of data points at large times and high temperature corresponds to time values close to the centre of the lattice which are contaminated by backward moving states. We have confirmed this interpretation by successfully modelling the effects of these backward moving states.

The central values for the potentials are obtained from  $\tau = 6, 7, 7, 7$  and  $24$  for  $N_T = 20, 24, 28, 32$  and  $80$  respectively. The resulting  $V_C$  and  $V_S$  are shown in Figs. 2 and 3. The left-hand error bars are statistical, and

the systematic uncertainty of choosing different values of  $\tau$  to define the potentials are depicted in the right-hand error bar. In Fig.2 we include the Cornell potential,  $V(r) = -\frac{\kappa}{r} + \frac{\tau}{a^2} + V_0$  with  $\kappa = 0.52$  and  $a = 2.34 \text{ GeV}^{-1}$  [24], as a point of reference.

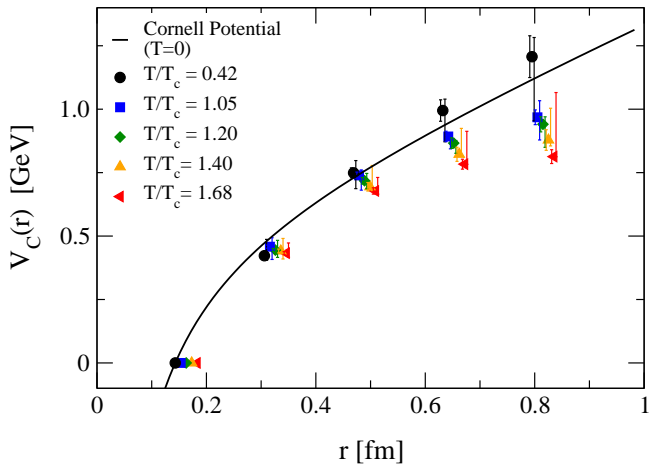


FIG. 2: Spin independent (i.e. central) potential,  $V_C(r)$ , for the temperatures in Table I obtained from eq.(6). The data points have been shifted horizontally for clarity. The solid curve is a fit to the Cornell potential [24] (see text).

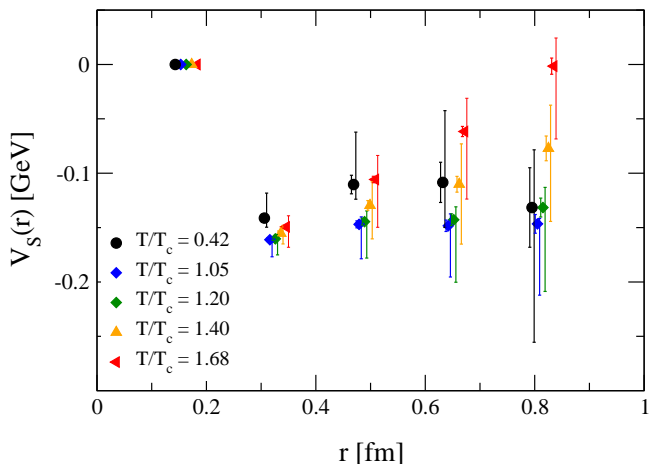


FIG. 3: Spin dependent potential,  $V_S(r)$ , for the temperatures in Table I obtained from eq.(6). The data points have been shifted horizontally for clarity.

From Fig.2 we see a clear temperature dependence. In the confined phase,  $T = 0.42T_c$ , we see evidence of a linearly rising potential in agreement with the Cornell potential. As the temperature increases beyond  $T_c$ , the potential flattens for large distances, in agreement with expectations of a deconfined phase. The spin dependent potential is plotted in Fig.3 and shows a repulsive core.

We now compare our results with those using static quarks. There are two general approaches to extract the interquark potential between static (infinitely heavy)

quarks, both of which have limitations. The first calculates the free energy of a static quark pair as a function of their separation via various correlators of Polyakov loops [13–15]. However, the potentials thus derived suffer from either gauge dependence (in the case of the “singlet” channel), or do not reduce to the correct Debye screened potential in the perturbative limit (in the case of the “averaged” channel) [15, 25]. The second uses Wilson loops or correlators of Wilson lines [15–17] and requires there to be good ground state dominance. However, this creates tension because the temporal extent of the lattice,  $N_\tau \sim 1/T$  is necessarily small at high temperature. As a result, precision results are difficult to obtain.

The method discussed here is gauge invariant by construction and produces results with reasonable systematics. Furthermore it calculates the potential between quarks with masses tuned to the physical charm.

In Fig.4 we compare our results from Fig.2 with those obtained from static quark calculations – the singlet free energy [14] and the Wilson loop and line [17]. We note a clear discrepancy between the our results and those obtained from static quarks.

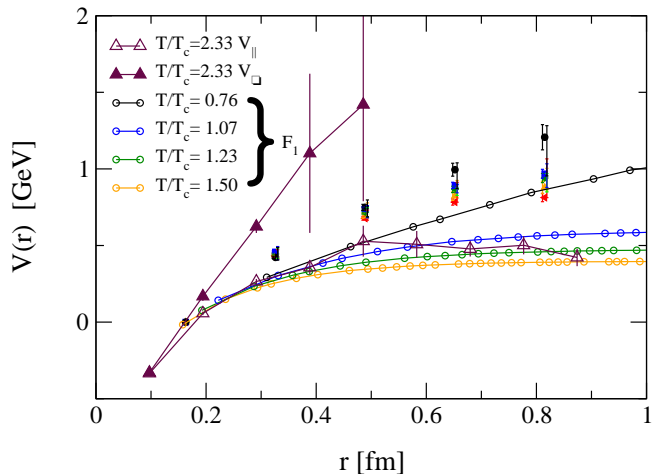


FIG. 4: Comparison of  $V_C$  from this work with the singlet free energy calculation,  $F_1$ , from [14] and the Wilson loop,  $V_\square$ , and Wilson line correlator,  $V_\parallel$ , from [17]. The error bars of the free energy data are smaller than the symbols. The data from this work follows the legend in Fig. 2.

*Conclusions* – There is a significant body of theoretical work studying the interquark potential at non-zero temperature using model, perturbative and lattice (non-perturbative) approaches. The work outlined here uses a lattice simulation of QCD with two light dynamical flavours on an anisotropic lattice. We determine the charmonium potential at a variety of temperatures using relativistic quarks tuned to the physical charm quark mass. This improves upon earlier lattice simulations performed in the static limit. It thus represents the first ab initio calculation of the charmonium potential of QCD at finite temperature.

The method we use is based on the HAL QCD “time-

dependent” approach which obtains the real part of the potential from correlators of point-split operators [19]. This allows the extraction of the potential without the need to first define the NBS wavefunctions by fitting the large time behaviour of the correlation functions.

Our determination of the potential shows a linearly rising potential for  $T < T_c$  and a clear temperature dependent flattening of the potential for  $T > T_c$ . We demonstrate a significant deviation between our results and those obtained using static quarks via either the free energy or Wilson loops/lines.

This work adds to previous charmonium studies performed by our collaboration with the same lattice parameters [23, 26] and our earlier work on the potential using the HAL QCD wavefunction method [21].

In forthcoming work we will simulate on significantly larger lattices with 2+1 light quark flavours. We also hope to extend our work to the potential between heavier

quarks using the NRQCD approach [27–29].

We acknowledge the support and infrastructure provided by the Trinity Centre for High Performance Computing and the IITAC project funded by the HEA under the Program for Research in Third Level Institutes (PRTLII) co-funded by the Irish Government and the European Union. The calculations have been carried out using CHROMA [30]. The work of CA and WE is carried as part of the UKQCD collaboration and the DiRAC Facility jointly funded by STFC, the Large Facilities Capital Fund of BIS and Swansea University. WE and CA are supported by STFC. CRA thanks the Galileo Galilei Institute for Theoretical Physics for hospitality and the INFN for support during the writing up of this work. We are very grateful to Gert Aarts, Sinya Aoki, Robert Edwards, Tetsuo Hatsuda, Balint Joó and Alexander Rothkopf for useful discussions.

- 
- [1] J. Adams *et al.* [STAR Collaboration], Nucl. Phys. A **757**, 102 (2005) [nucl-ex/0501009].
- [2] K. Adcox *et al.* [PHENIX Collaboration], Nucl. Phys. A **757**, 184 (2005) [nucl-ex/0410003].
- [3] KÅamodt *et al.* [ALICE Collaboration], Eur. Phys. J. C **65**, 111 (2010) [arXiv:0911.5430 [hep-ex]].
- [4] T. Matsui and H. Satz, Phys. Lett. B **178**, 416 (1986).
- [5] P. Braun-Munzinger and J. Stachel, Phys. Lett. B **490**, 196 (2000) [nucl-th/0007059].
- [6] P. Braun-Munzinger and J. Stachel, Nucl. Phys. A **690**, 119 (2001) [nucl-th/0012064].
- [7] Y. -P. Liu, Z. Qu, N. Xu And P. -F. Zhuang, Phys. Lett. B **678**, 72 (2009) [arXiv:0901.2757 [nucl-th]].
- [8] X. Zhao and R. Rapp, Nucl. Phys. A **859**, 114 (2011) [arXiv:1102.2194 [hep-ph]].
- [9] S. Chatrchyan *et al.* [CMS Collaboration], Phys. Rev. Lett. **107**, 052302 (2011) [arXiv:1105.4894 [nucl-ex]].
- [10] R. Reed, J. Phys. G **38**, 124185 (2011) [arXiv:1109.3891 [nucl-ex]].
- [11] F. Karsch, M. T. Mehr and H. Satz, Z. Phys. C **37**, 617 (1988).
- [12] Y. Burnier, M. Laine and M. Vepsäläinen, JHEP **0801**, 043 (2008) [arXiv:0711.1743 [hep-ph]], N. Brambilla, J. Ghiglieri, A. Vairo and P. Petreczky, Phys. Rev. D **78**, 014017 (2008) [arXiv:0804.0993 [hep-ph]], A. Dumitru, Y. Guo, A. Mócsy and M. Strickland, Phys. Rev. D **79**, 054019 (2009) [arXiv:0901.1998 [hep-ph]].
- [13] O. Kaczmarek, F. Karsch, F. Zantow and P. Petreczky, Phys. Rev. D **70**, 074505 (2004) [Erratum-ibid. D **72**, 059903 (2005)] [hep-lat/0406036], Y. Maezawa *et al.* [WHOT-QCD Collaboration], Phys. Rev. D **75**, 074501 (2007) [hep-lat/0702004], A. Mócsy and P. Petreczky, Phys. Rev. D **77**, 014501 (2008) [arXiv:0705.2559 [hep-ph]], Z. Fodor, A. Jakovác, S. D. Katz and K. K. Szabo, PoS LAT **2007**, 196 (2007) [arXiv:0710.4119 [hep-lat]], P. Petreczky, C. Miao and A. Mócsy, Nucl. Phys. A **855**, 125 (2011) [arXiv:1012.4433 [hep-ph]]. A. Bazavov and P. Petreczky, arXiv:1210.6314 [hep-lat].
- [14] O. Kaczmarek and F. Zantow, Phys. Rev. D **71**, 114510 (2005) [hep-lat/0503017].
- [15] A. Bazavov and P. Petreczky, arXiv:1211.5638 [hep-lat].
- [16] A. Rothkopf, T. Hatsuda and S. Sasaki, PoS LAT **2009**, 162 (2009) [arXiv:0910.2321 [hep-lat]], A. Rothkopf, T. Hatsuda and S. Sasaki, Phys. Rev. Lett. **108**, 162001 (2012) [arXiv:1108.1579 [hep-lat]].
- [17] Y. Burnier and A. Rothkopf, Phys. Rev. D **86**, 051503 (2012) [arXiv:1208.1899 [hep-ph]].
- [18] Y. Ikeda and H. Iida, PoS LATTICE **2010**, 143 (2010) [arXiv:1011.2866 [hep-lat]], Phys. Rev. Lett. **107**, 091601 (2011) [arXiv:1102.3246 [hep-lat]], T. Kawanai and S. Sasaki, Phys. Rev. D **85**, 091503 (2012) [arXiv:1110.0888 [hep-lat]], PoS LATTICE **2011**, 126 (2011) [arXiv:1111.0256 [hep-lat]], PoS LATTICE **2011**, 195 (2011).
- [19] N. Ishii, S. Aoki and T. Hatsuda, Phys. Rev. Lett. **99**, 022001 (2007) [nucl-th/0611096], S. Aoki, T. Hatsuda and N. Ishii, Prog. Theor. Phys. **123**, 89 (2010) [arXiv:0909.5585 [hep-lat]], S. Aoki *et al.* [HAL QCD Collaboration], arXiv:1206.5088 [hep-lat].
- [20] N. Ishii [HAL QCD Collaboration], PoS LATTICE **2011**, 160 (2011).
- [21] C. Allton, W. Evans and J. -I. Skullerud, PoS LATTICE **2012**, 082 (2012).
- [22] R. Morrin, A. Ó Cais, M. Peardon, S. M. Ryan and J. -I. Skullerud, Phys. Rev. D **74**, 014505 (2006) [hep-lat/0604021].
- [23] M. B. Oktay and J. -I. Skullerud, arXiv:1005.1209 [hep-lat].
- [24] E. Eichten, K. Gottfried, T. Kinoshita, K. D. Lane and T. -M. Yan, Phys. Rev. D **21**, 203 (1980).
- [25] O. Jahn and O. Philipsen, Phys. Rev. D **70**, 074504 (2004) [hep-lat/0407042], O. Philipsen, Nucl. Phys. A **820**, 33C (2009) [arXiv:0810.4685 [hep-ph]].
- [26] G. Aarts, C. Allton, M. B. Oktay, M. Peardon and J. -I. Skullerud, Phys. Rev. D **76**, 094513 (2007) [arXiv:0705.2198 [hep-lat]].
- [27] G. Aarts, S. Kim, M. P. Lombardo, M. B. Oktay, S. M. Ryan, D. K. Sinclair and J. -I. Skullerud, Phys. Rev. Lett. **106**, 061602 (2011) [arXiv:1010.3725 [hep-lat]].

- [28] G. Aarts, C. Allton, S. Kim, M. P. Lombardo, M. B. Oktay, S. M. Ryan, D. K. Sinclair and J. I. Skullerud, *JHEP* **1111**, 103 (2011) [arXiv:1109.4496 [hep-lat]].
- [29] G. Aarts, C. Allton, S. Kim, M. P. Lombardo, M. B. Oktay, S. M. Ryan, D. K. Sinclair and J. -I. Skullerud, *JHEP* **1303** 084 (2013) [arXiv:1210.2903 [hep-lat]].
- [30] R. G. Edwards and B. Joó [SciDAC and LHPC and UKQCD Collaborations], *Nucl. Phys. Proc. Suppl.* **140**, 832 (2005) [hep-lat/0409003].
- [31] Only on-axis separations were studied in this work.